Scientific Papers Series Management, Economic Engineering in Agriculture and Rural Development
Vol. 24, Issue 3, 2024
PRINT ISSN 2284-7995, E-ISSN 2285-3952

USING REMOTE SENSING TECHNIQUES TO ESTIMATE ACTUAL EVAPOTRANSPIRATION IN THE NILE DELTA, EGYPT

Asaad DERBALA[1], Darwish MOHAMED[1], Hesham ABOELSOUD[2], Abdel Aziz BELAL[3], Abdallah ELASSAL[1], Mayie AMER[1]

[1]Tanta University, Faculty of Agriculture, Agriculture Engineering Department, Egypt, E-mails: asaadderbala@yahoo.com, rmdarwish@yahoo.com, abdallahmohamedomar30@gmail.com, mayieamer@yahoo.com
[2]Soils, Water and Environment Research Institute, Agricultural Research Center, Egypt, E-mail: hm_aboelsoud@yahoo.com
[3]National Authority for Remote Sensing and Space Sciences. Agricultural Applications, Soil and Marine Science Division, Egypt, E-mail: abelal@narss.sci.eg

Corresponding author: asaadderbala@yahoo.com

Abstract

With 755 million tonnes consumed as a cereal grain in 2020, rice is the most consumed crop in the world. Estimating rice's water requirements is crucial since the crop often grows under flood conditions and water serves a number of vital purposes for it. This study uses the Penman-Monteith (FAO 56-PM) method to assess and estimate evapotranspiration, whereas the METRIC model is used to calculate surface enrage balance. The estimation and monitoring of field agricultural water use has shown to be a successful application of remote sensing technology. Using remote sensing techniques, this work aimed to develop a method for estimating crop coefficient and actual crop evapotranspiration (ETc). for rice using METRIC model within the Google Earth Engine (GEE) based on Landsat-8 satellite imagery. The average seasonal ETo (FAO56) resulted 469 mm for crop rice and the water productivity (WP) was 0.42 kg m-3. Good correlations were found between the crop coefficients (Kc) proposed by FAO and (Kc) sat, with R^2 0.92. The Kc_{FAO} used to validate Kc_{Sat}. Linear relationship between Kc_{FAO} and Kc_{Sat} was established and R^2 was 0.96. Normalized Deference Vegetation Index (NDVI) used to estimate crop coefficient according to satellite data (Kc_{Sat}). Landsat TM and Landsat ETM+ data were used to outline the growth of vegetation cover, and these data were coupled with land surface temperature (LST) taken from Landsat8 satellite data and air temperature (Tair) acquired from ground stations. The findings indicated that as cultivated area expanded during rice development, (LST) declined by around 2.3°C and (Tair) reduced by roughly 1.6°C.

Key words**:** *Evapotranspiration (ET0),water productivity (WP), Land Surface Temperature (LST), crop coefficient (Kc), remote sensing*

INTRODUCTION

Rice is generally recognized as the most important crop for human sustenance since it feeds more than half of the world's population and is the most commonly consumed cereal grain [5]. Due to its lower production costs compared to other summer field crops like maize, cotton, and rice is Egypt's most significant crop in the Nile Delta. About 50% of Egyptians depend on it as their primary source of sustenance, particularly in the Nile Delta and Northern Egypt [8]. According to the Ministry of Agriculture, Egypt's 510,649 acres of rice field produced 326,429 tons of rice in 2015 [10]. A total of 1,100–1,500 mm of water are needed for the rice crop [11, 32]. Comparing this amount to other grain crops throughout the growing season, it is considered to be significant. The mechanism of evapotranspiration is essential to the water cycle. It contributes around 15% of the water vapour atmosphere. The absence of it would result in a significantly colder atmosphere and reduced precipitation. Conversely, nevertheless, the expression Conversely, the term "water productivity" describes the proportion of crop production, or agricultural output, to water intake. Stated differently, it assesses the effectiveness of water usage in farming. Usually, it is stated as the volume of water used to produce one unit of agricultural output. Increasing water productivity is essential for sustainable agriculture,

particularly in areas with little water resources. It requires undertaking tasks including improving irrigation efficacy, choosing drought-resistant agricultural varieties, and implementing improved water management strategies. Understanding both evapotranspiration and water production is crucial for efficient management of water resources, especially considering climate change and increasing water shortages.

This is due to the fact that additional factors related to water use, such as percolation (the vertical movement of water in the soil beyond the root zone), lateral flow losses, and surface drainage are taken into account in addition to evapotranspiration, which takes into account both water evaporation and plant transpiration. Rice has a water use efficiency that is comparable to other cereals when just evapotranspiration is taken into consideration [33, 26]. The Food and Agricultural Organisation of the United Nations (FAO) divides the reference evapotranspiration (ETo) by the crop coefficient (Kc) to determine the actual evapotranspiration (ETa) of a given crop [2]. Since ETa is a crucial component of the decision support tools used in field management, it is necessary to construct effective irrigation systems at the field size. Understanding the hydrological cycle, which is directly impacted by global warming, is further aided by the measurement of ETa [31]. Numerous investigations have concentrated on determining Kc using crops experimentally measured ET. The relationships between variations in leaf area, plant height, crop features, irrigation technique, crop development rate, crop planting date, canopy cover %, canopy resistance, soil and environmental variables, and management techniques are illustrated by the Kc values [23]. Applications for the single- and dual-crop coefficient techniques are many. The impacts of soil evaporation and crop transpiration are combined into a single coefficient known as the single crop coefficient [20]. On the other hand, the soil surface evaporation is represented by the coefficient of transpiration and soil evaporation (Ke), whereas the dual crop coefficient indicates Kc. According to Allen and others [2]. The dual crop factor is typically used in research, real-time irrigation scheduling, additional irrigation scheduling, and in-depth analyses of the soil balance and hydrologic fluid. The single crop coefficient is utilised for irrigation planning and design, basic and real-time scheduling of shorter-term water applications, and irrigation management. These researchers used both single-crop and dual-crop techniques to present the crop coefficients of various crops grown with unlimited irrigation, noting that Kc can be affected by soil evaporation, crop type, atmospheric variables (like rainfall, wind velocity, and relative humidity), as well as the growth of the crops [22]. Despite several attempts to establish it empirically for numerous crops, regional variability in Kc is very challenging to define. This is due to the fact that it depends on several management inputs such as irrigation techniques, soil moisture, the availability of nutrients, and plant morphological traits, as well as variables such as climate, soil type, crop type, and variety [2; 15]. An option to determining Kc by employing vegetative indices (VIs) generated from satellite data is the Remote Sensing (RS) approach. One of the most used vegetation indexes in agriculture is the Normalised Difference Vegetation Index (NDVI). While soil reflectivity and the saturation effect may have an effect on the NDVI [29]. The primary cause of selecting this index was to maintain the consistency of past investigations that have been reported in the scientific literature [13,11]. This index benefits from the high reflectance of plant materials in the red spectrum channel (0.62-0.69 m) and the NIR band (0.75-1.3 m). pigments from chloroplasts absorbed. (NIR RED)/(NIR + red) is the normalised ratio of the red and NIR wavelength bands, which is used to construct the index [30,14]. Since increased levels of photosynthetic activity lead to Smaller reflectance coefficient values in the red area of the spectrum and large values in the NIR region allow for a clear separation between vegetation and several other natural components. NDVI normally falls between 0.1 and 0.2 for bare ground and between 0.2 and 1 for vegetation. This is because vegetation has a strong NIR reflection and a low red band reflectance [34].

The NDVI, which helps with the study of the dynamics of the vegetation during the growth season, is closely connected with plants' ability to employ photosynthetic activities to absorb energy [25]. The capacity to keep an eye on changes in the vegetation during the growth season is made possible by the NDVI, which is directly related to plant canopies' capability for photosynthesis and energy absorption [19]. In a separate experiment, Kc was calculated using a linear correlation between Kc and VI, the linear connection between Kcb and VI, a calibrated model of Kc-VI, and a verified model of Kcb-VI based on Landsat 7 data. The findings demonstrated that variations in the NDVI across all techniques could adequately account for variations in Kc [21]. It is possible to produce ETc maps at various scales using remote-sensing-based estimations of ET was calculated using Surface Energy Balance models based on multispectral satellite images [3, 27]. Among the several surface energy balance models, METRIC (Mapping Evapotranspiration at High Resolution with Internalised Calibration) [4].

The aims of this paper were to estimate Eta using Landsat data in summer season 2022, and bio physical variables such.as NDVI, LST, surface albedoand surface emissivity wh ich are useful for the estimation of spatiotemporalvariations in evapotranspiration (ET) using METERIC model and FAO56.

MATERIALS AND METHODS

The study area has a dry arid climate, according to the Köppen Climate Classification System, with rainfall being less than 50 % of the region's estimated evapotranspiration. The location of its UTM coordinates is between latitudes 31° 6′ 10.89 " N to 31° 4′ 7.10" N and 31° 5′ 57.85" E to 30° 59′ 56.16" E.

The whole study area is about 997ha.

A uniform clay-silt soil with a high clay content and low organic matter (1.2%), the soil in the study region has a field capacity of 44 % and a permanent wilting point of 21% and a Mediterranean climate with hot, dry summers and cool, wet winters characterize the research region.

As showed in Fig. 1, this study was conducted in El-Gharbia main drain irrigated area in the Kafr El-Sheikh governorate of Egypt's North Nile Delta.

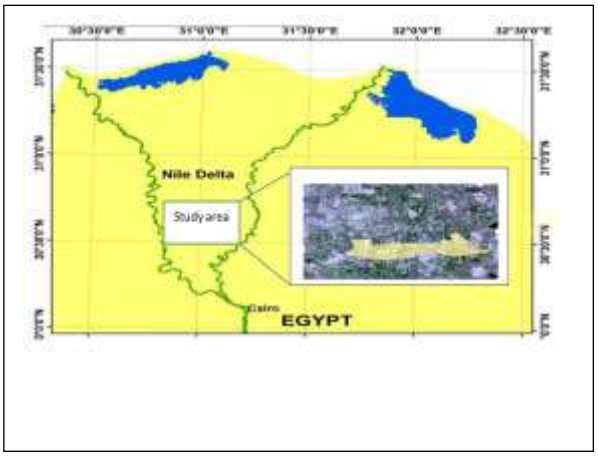

Fig. 1. Location Map of the studied area
Source: designed by authors.

The average yearly temperature is around 19° C.

The annual average rainfall is about 22 mm. The month of January typically records the highest rainfall totals (7 mm on average).

The month with the highest average high temperature is Aug (40 C), while the coldest month on record is January (12 C).

The minimum temperature varies from 12 °C in January to 21 °C in August.

Table 1. meteorological data in 2022 for Kafr El-Sheikh

Month	Min Temp. ° C	Max Temp. ° C	Wind speed km/h	Relative humidity %	ETo monthly
June	19.9	38	6.7	44	232
July	20	39	4.3	50	284
August	20	40	2.2	55	469
September	19	38	2.3	56	327
October	17	37	2.7	57	258
November	11.7	25.3	2.7	89	200
December	7.5	20.9	3.1	84	110
January	7.58	19.23	4.2	80.6	68
February	8.5	20.5	4.9	89.5	86
March	12.4	24.6	4.7	81.5	84
April	16.4	26.4	4.4	75.8	100
May	19.8	31.4	5.3	72.9	127

Source: Data from Sakha Station.

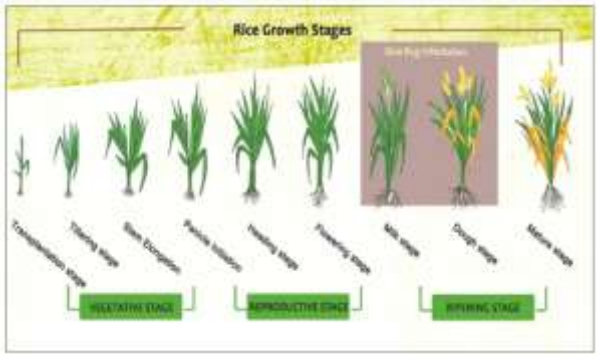

Fig. 2. Rice crop growth stages
Source: Own conception.

Remote Sensing Data Availability

The Landsat 8 data (path 176/row 039) with a 30 meter ground resolution that was acquired during the summer at 10 a.m. The Sallite images were collected on July 26, 2022, August 11, 2022, August 27, 2022, and September 19, 2022. The majority of the study's data came from GEE collecting using Python.

Landsat 8 satellite data were used to calculate NDVI. The United States Geological Survey (USGS) contributed images captured by the Landsat satellite, which is equipped with a functional land imager (OLI) and a thermal infrared sensor (TIRS). A thermal infrared sense (TIRS) with a resolution of 100 m and an operational land imager (OLI) with a resolution of 30 m make up Landsat pictures, which are frequently utilized for managing water resources. The program releases Albedo, vegetation index, land surface temperature, and other surface data are used in conjunction with Landsat's thermal and shortwave channels to calculate ETa [28].

Crop coefficient

Due to differences in evapotranspiration throughout various growth stages, the Kc for a certain crop varies at the growing season. The rice season of cultivation was divided into main three distinct growing stages: Fig. 2 shown the rice growth stages are vegetative stage, reproductive stage, and ripening stage. The Kc curve must be constructed using three typical Kc values: Kc- Veg at the start of the season, Kc-rep.at midseason, and Kc-Rip at late season's finish. According to the FAO-56 method's recommendations, under a typical climatic condition, Kc-Veg., Kc-Rep., and Kc-Rip should be 1.05, 1.2, and 0.9, respectively [2]. It is clear that NDVI and Kc are related. Due to parallels between the Kc curve and a vegetation index generated from satellite data, modelling Kc as a function of vegetation index shows potential. Therefore, it was investigated to see if Kc could be directly estimated from a crop's satellite reflectance [6]. The formula below can be used to generate NDVI data using Landsat8 bands 4 and 5, which provide R and NIR measurements such as:

NDVI = (Band 5 - Band 4) / (Band 5 + Band 4)…….....(1)

Kc is combined with ETo to estimate ETc. The value that is calculated (ETc) is obtained by multiplying the dimensionless number Kc by the ETo value, which normally lies between 0.1 and 1.2. The produced ETc can be used by an irrigation manager to schedule when to irrigate and how much water needs to be returned to the land. The link between Kc_{Sat} and NDVI is represented by the equation.

$$Kc_{Sat}=\frac{1.02}{0.6}(NDVI-0.2) \quad \ldots\ldots\ldots\ldots \quad (2)$$

where: 1.02 is the greatest Kc for rice under Egyptian environment; 0.2 is the smallest NDVI value for vegetation; and 0.6 is the variance across the minimum and maximum NDVI value for vegetation.

Crop evapotranspiration

According to Jenson's proposed equation [16], the actual crop water use was calculated:

$$ETa=ETo\times K \quad \ldots\ldots\ldots\ldots\ldots\ldots \quad (3)$$

Meteorological data were utilised to compute ETo using the FAO-Penman-Montieth method. The aforementioned equation was created using an empirical approach to estimate ETo. The crop coefficient (kc) was then added to obtain ETc. The Sakha meteorological station provided the meteorological characteristics utilised in this calculation. The equation that was applied was:

$$ETo=\frac{0.408\Delta(R_n-G)+\gamma\left[\frac{900}{T+273}\right]U_2(e_s-e_a)}{\Delta+\gamma(1+0.3442U_2)} \ldots\ldots\ldots(4)$$

where: Rn, the net radiation at the crop surface [MJ m-2 day-1], and ETo, the reference evapotranspiration [mm day-1], G, the density of soil heat flow (MJ m-2 day-1) U2, or wind speed at a height of two metres, and T, or mean daily air temperature at two metres [°C] Δ, slope vapour pressure curve [kPa °C-1],γ, psychrometric constant [kPa °C-1], es, saturation vapour pressure [kPa], ea, actual vapour pressure [kPa], and es - ea, saturation vapour pressure deficit [kPa]. The land surface temperature (LST) is calculated using equations:

$$T = T_{61} + [1.29 + 0.28(T_{61} - T_{62})](T_{61} - T_{62}) + 45(1 - \varepsilon_4) - 40\Delta\varepsilon \dots (5)$$

$$\varepsilon_4 = 0.9897 + 0.029 \ln(NDVI) \dots \dots . (6)$$

$$\Delta\varepsilon = 0.01019 + 0.01344 \ln(NDVI) \dots \dots . . (7)$$

where: T_{61} , T_{62} are the brightness temperature of the thermal bands (T_{61} and T_{62}) of remote sensing data, ε_4 the surface emissivity of T_{61} channel, and $\Delta\varepsilon$ is the differences in surface emissivity between the T_{61}, T_{62} channels.

Water productivity (WP)

Water productivity is defined as the field obtained per unit of water applied. Water productivity was calculated using the following equation:

$$\text{WP } (\frac{\text{kg}}{\text{m}^3}) = \frac{\text{Y}}{\text{WR}} \dots \dots \dots \dots \dots \dots \dots \dots \dots (8)$$

where:
Y= yield (kg.fed^{-1}), and
WR= the total amount of water applied in the field (m^3.fed^{-1}) to determine the rice and wheat 1m^2 of plants per each plot were harvested manually.

RESULTS AND DISCUSSIONS

The daily reference evapotranspiration for Penman-Monteith rice ranged from 4 to 15 mm day-1. August was the month with the highest daily ETo levels, as the temperature, sun radiation, and VPD were at their highest levels. Daily From May until August, ETo increased before declining in the last months of the year. ETo daily values ranged from 6 to 15 mm day^{-1} from tillering to maturity stages, respectively. The maximum values in booting and elongation ranged from 216 to 200 mm for ETo monthly values. For sustainable water management and to apply agricultural A study on long-term developments in climatic parameters should be suggested within the context of changing climates in order to preserve and advance food production in a research area under water shortage.

NDVI

Figure 3 shows the NDVI values at different growth stages.

In 2022, the difference between the five stages was more noticeable for the first two stages. At the end of July (Tillering stage), the NDVI values ranged between 0.21 to 0.35. At the beginning of August, the curve intersected, showing a homogeneous distribution. The NDVI decreased towards the end of September after reaching its peak in the middle of the month (about 0.83). The NDVI curve stayed superposed, peaking at the end of August at around 0.80. In 2022, it stayed almost exactly overlapping for the duration of the cultural cycle. Up to the end of August, the NDVI displayed a higher level of vegetative vigour (the whole first phase). At heading 29, the NDVI peak (between 0.78 and 0.83) was attained for all the plants as showed Figure 3.

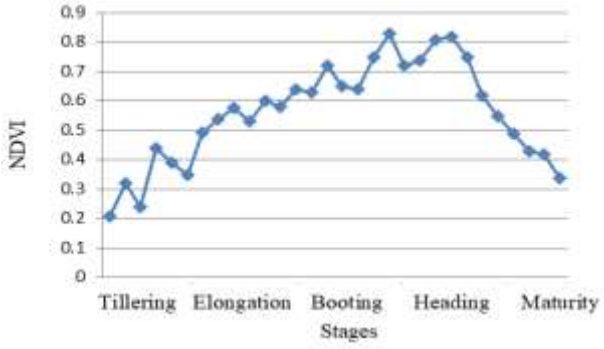

Fig. 3. NDVI for different rice growth stages.
Source: Own research results.

The first rice crop cultivation stage produced the lowest NDVI values (less than 0.3), which were attributed to plant flooding. The greatest NDVI values, around 0.75 and 0.83, were attained in the middle phase, which also reflects the various sowing dates, at the conclusion of booting and the start of heading, respectively. As the growing season came to a

conclusion, the NDVI values dropped until the plant was fully mature and harvested at the end of September.

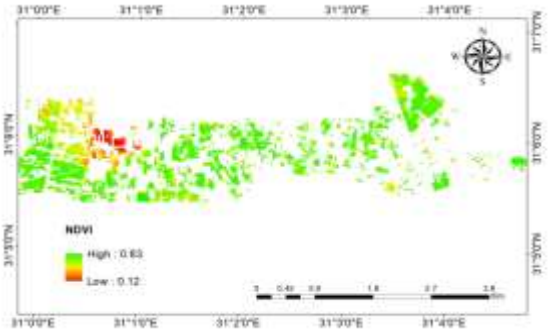

Fig. 4. NDVI extracted from Landsat 8 in heading stage
Source: Own research results.

Land surface temperature and Air Temperature

Due to specific physical factors, the relationship between Temperature of air (T-air) and LST in the thermodynamics of the biosphere is always rather elusive. This relationship was applied to forecast T_{air} from LST as showed Table 2. LST at night was lower than Tair, however on the day it was the opposite due to the increased surface emitted energy, wind speed, and air humidity affecting T_{air}. The relation between LST and T_{air} is positive relationship where the slope is 0.3946, the intercept is 16.327 and R^2 is 0.87 as showed in Fig. 5 and 6.

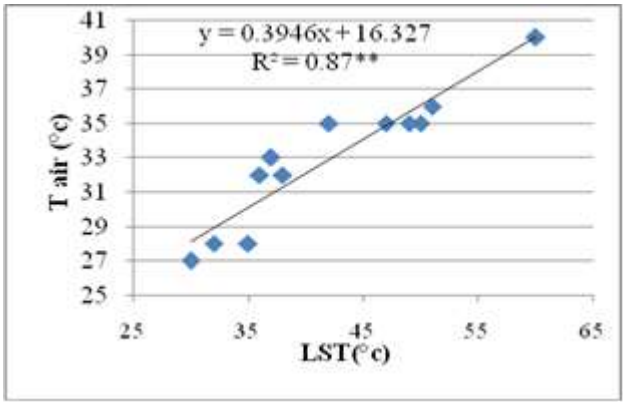

Fig. 5. Relationship between Land surface temperature and air temperature (excel)
Source: Own research results.

Table 2. Illustrates KcSat and Kc FAO simple model description

Model	Unstandardized Coefficients		Standardized Coefficients	t	Sig.
	B	Std Eror	Beta		
(Constant)	.015	.087		0174	.873
Kc FAO	1.034	.110	.983	9.412	.003

Source: Own research results.

Kc coefficient

The canopy height, crop development, layout, and plant cover affect Kc [2]. The NDVI was correlated to Kc in a positive. The Red and NIR bands of the Landsat8 data were used to calculate NDVI of landsat8 data acquired on 26 Jul, 11 Aug, 27 Aug,12 sept and 28 sept respectively.

Figure 6 shows the variation in Kc values in the study region based on Landsat8 data. Kc varied in the sample area from 0.6 to 1.02 as showed in Table 3.

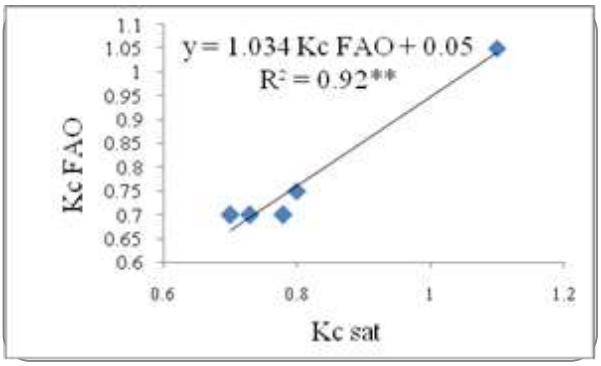

Fig. 6. Relationship between Kc sat and Kc FAO.
Source: Own research results.

There is a strong correlation between Kc and NDVI. Because empirical Kc values vary depending on the environment and crop stage in which they were derived, they have faced criticism for their significance and applications. When the regression strength of the association between the two variables is analyzed, the diagram shows that the developed model has a significant correlation between the Kc Sat and Kc FAO, as showed in Fig. 7.

The model parameters are shown in Table 2, R^2 value is 0.92. The method we present in this study is based on the calibration of the equation shown below.

Kc sat= $\frac{1.02}{0.6}$(NDVI-0.2) equation.

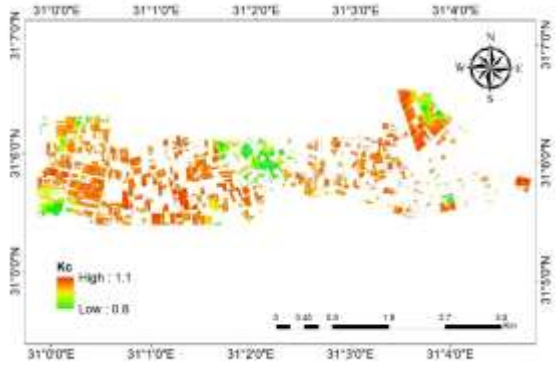

Fig. 7. Kc various in different sites for booting.
Source: Own research results.

It was adjusted for our specific rice crop and local conditions with the goal of further applying it to a temporal series of satellite photographs and replicating a range of crop scenarios under varying management approaches, resulting in a diversity of ETa values. Figure 8 shows a comparison between the ETosat values and estimated EToFAO from methodologies, for the dates with availabilities of Landsat 8 images, for the five campaigns. The satellite derived NDVI data effectively captures this variability. The FAO56 methodology, which assigns uniform crop coefficient for all plants or surface conditions without making a distinction based on planting dates, does not take this into consideration.

Rice actual evapotranspiration (ETc)

Evapotranspiration accounts for the biggest flux in the hydrological cycle, and as data collection is essential for assessing land-use governance and predicting how plants will respond to climate change, daily estimates of ET are important for managing water resources. It's vital to remember that evapotranspiration is influenced by a range of environmental conditions and plant features, such as plant morphology and growth stage. For 2022, ETc daily growth stages varied from 4 to 15 mm, with booting stages having a greater value of 15 mm. ETc monthly growth stages ranged between 129.7 to 467.2 mm for 2022 which was higher value467.2 mm for booting stage, Lower value 129.7 mm for Tillering stage because high the atmosphere evaporative demand was brought on by conditions of high sun radiation, temperatures, and vapor pressure deficit as well as by the plant's steady growth, which makes it consume more water as the temperature rises towards August. Conversely, low the atmosphere evaporative demand was brought on by conditions of low sun radiation, temperatures, and VPD as well as by the plant's steady growth, which makes it utilize less water as the temperature increases towards August as a showed Fig. 9, Fig. 10 and Table 3.

Contrarily, throughout the vegetative and reproduction phases of the crop and decreased during the maturity phase during the WS, the actual daily evapotranspiration of rice altered less. Data also revealed that the ETc peaked in August before declining till harvest. The existing agronomic and meteorological conditions may have caused these results [17, 18, 1].

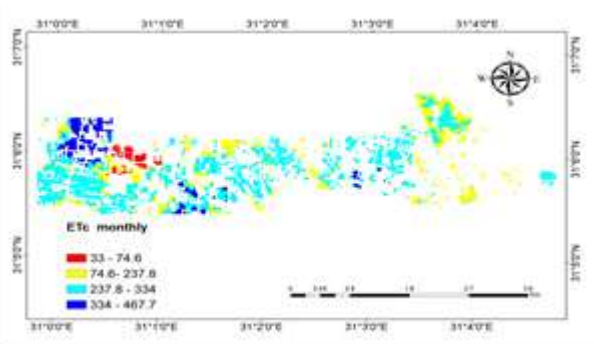

Fig. 8. Monthly actual evapotranspiration Booting stage extracted from Landsat 8.
Source: Own research results.

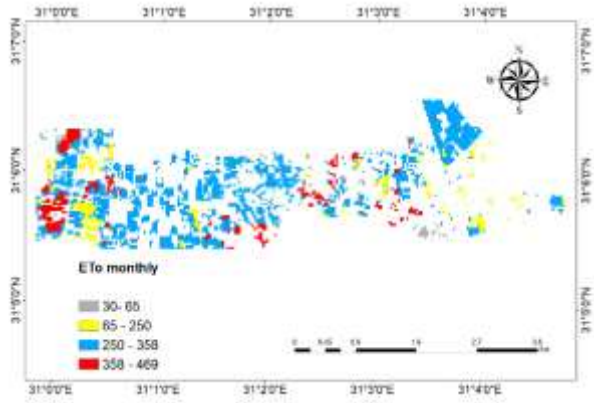

Fig. 9. Monthly evapotranspiration for Elongation stage extracted from Landsat 8.
Source: Own research results.

Table 3. Evapotranspiration and Kc coefficient at the experimental site for rice for different growth stages

Stages	ETo daily	ETo monthly	ETc daily	ETc monthly	Kc
Tillering 26/July	6.4-8.6	216-284	4.1-5.4	129.7-170.4	0.70
Elongation 11/August	11-15	358-469	9-11.8	281-366.3	0.78
Booting 27/August	9-13	301-425	10.7-15	334-467.2	1.02
Heading 12/September	5.7-7.7	193-258	5.7-7.7	173-232	0.9
Maturity 28/September	6.9-10.9	207-327	4.8-7.6	146-229.2	0.7

Source: Own research results.

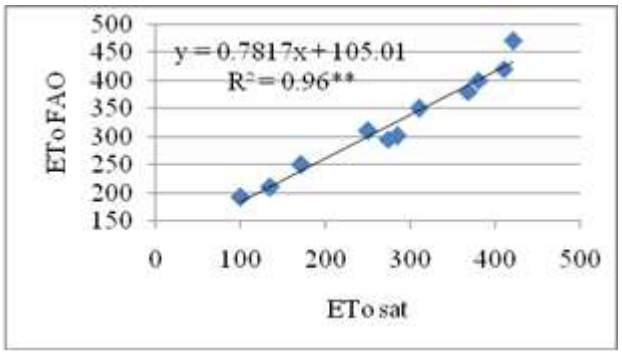

Fig. 10. Relationship between ETo FAO and EtosatSource: Own research results.

Land surface temperature and Air Temperature

Due to specific physical factors, the relationship between Temperature of air (T-air) and LST in the thermodynamics of the biosphere is always rather elusive. This relationship was applied to forecast T_{air} from LST as showed in Table 4.

Table 4. Water productivity and land surface temperature (LST) at the experimental site for rice

Stages	**WP m^3/ton**	**LST**
Tillering	1.1	24-28
Elongation	0.7	33-39
Booting	0.4	24-27
Heading	0.8	22-27
Maturity	0.9	26-28

Source: Own research results.

LST at night was lower than Tair, however on the day it was the opposite due to the increased surface emitted energy, wind speed, and air humidity affecting T_{air}.

The relation between LST and T_{air} is positive relationship where the slope is 0.3946, the intercept is 16.327 and R^2 is 0.87as a showed Fig. 11 and Fig. 12.

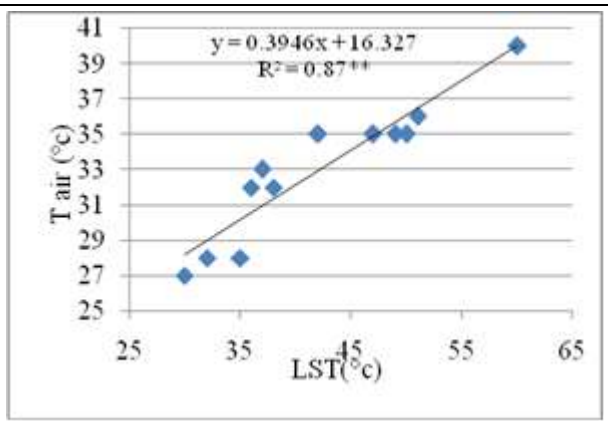

Fig. 11. Relationship between Land surface temperature and air temperature
Source: Own research results.

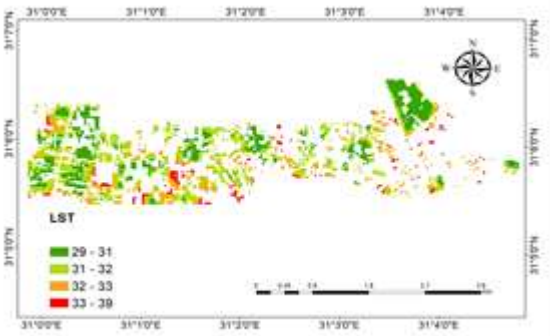

Fig. 12. Land surface temperature (LST) °C, Elongation extracted from Landsat 8
Source: Own research results.

Crop Production and Productivity of Irrigation Water

A comparison of the rice yield (kg/fed) and WP (kg/m3) may be shown in Figure 13. The yield outcomes are related to the amount of water used. It was feasible to link both factors to determine the WP after samples of mature plants were gathered and examined. For each of the rice growing seasons, the findings produced with the ETo sat technique matched the predicted ETc from the FAO56 extremely well. In 2022, there was a larger yield of rice grains. (4.9t/fed), the lowest and higher WP were (0.41, 0.53) Kg/m^3. A WP of rice of around 0.4 kg/m3 has been observed by certain researchers based on the total water input (rainfall + irrigation) [9]. These statistics (an average value of 0.47 kg/m3) are consistent with those found in the current investigation. Reaching this WP challenge may be accomplished in one of two ways: (i) by increasing crop production while lowering applied water usage, or (ii) by

increasing productivity (growing crop yield) while using the same quantity of water. According to Blatchford et al. [7], the first approach is preferable for developing strategies for lowering water usage while preserving food production at the basin size where water is the top issue. Farmers ought to be urged to save water if the objective is to lower the amount used. But regardless of the effects on the environment, farmers—especially smallholders with difficult financial circumstances—generally prefer to focus on yields over water use [24].

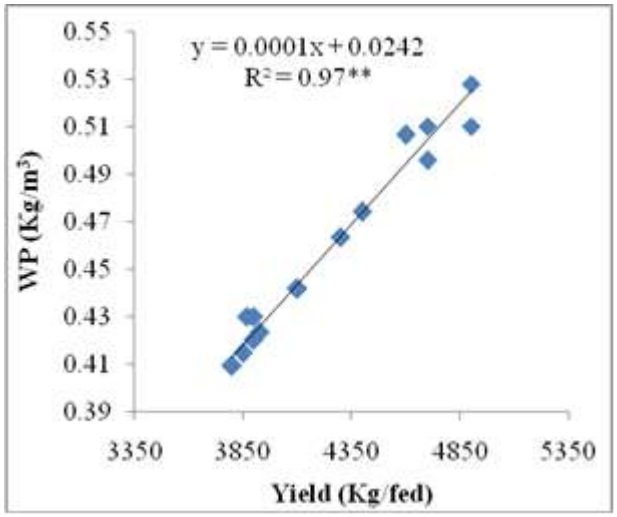

Fig. 13. Relationship between Yield (Kg/fed) and WP (Kg/m^3)
Source: Own research results.

CONCLUSIONS

In order to evaluate the effect of the growth of agricultural areas on the air temperature, a case study in KafrElshiekh was conducted. LST, NDVI, Yield, and Kc were generated using data from Landsat 8. To evaluate LST, tair data from Sakh ground station were used. The research of ETo allowed for a thorough investigation of the water condition of the plants over the study period, ETc and WP. The WP boundaries in each district reveal that there is great potential to improve water use efficiency and productivity. $Kc_{Sat} = \frac{1.02}{0.6}(NDVI - 0.2)$ represented the relation between crop coefficient (Kc) and NDVI.

Linear relationship between KcFAO and KcSat was established (y = 1.034 Kc FAO + 0.05) and R^2 was 0.92. Crop actual evapotranspiration (ETc) varied from 129.7 to 469.7 mm with the highest ETc obtained during the hot and dry seasons. The results of this study can be used as a guideline for rice water use and irrigation water requirement by the irrigation designers, agricultural project managers, consultants, universities, producers, and other stakeholders within rice value .

REFERENCES

[1]Abdullahi, A. S., Soom, M.A.M., Ahmad, D., Shariff, A.R.M., 2013, Characterization of rice (Oryzasativa) evapotranspiration using micro paddy lysimeter and class "A" pan in tropical environments. Australian Journal of Crop Science 7(5):650-658.

[2]Allen, R.G., Pereira, L.S., Raes, D., Smith, M.,1998, Crop Evapotranspiration-Guidelines for Computing Crop Water Requirements-FAO Irrigation and Drainage Paper 56. FAO, Rome, 300, D05109.

[3]Allen, R., Irmak, A., Trezza, R., Hendrickx, J.M.H., Bastiaanssen, W., Kjaersgaard, J., 2011 Satellite-based ET estimation in agriculture using SEBAL and METRIC. Hydrol. Process. 25, 4011–4027. [CrossRef]

[4]Allen, R.G., Tasumi, M., Trezza, R., 2007, Satellite-Based Energy Balance for Mapping Evapotranspiration with Internalized Calibration (METRIC)—Model. J. Irrig. Drain. Eng. 133, 380–394. [CrossRef]

[5]Awika, J.M., 2001, Major Cereal Grains Production and Use around the World. In Advances in Cereal Science: Implications to Food Processing and Health Promotion; ACS Symposium Series 1089; American Chemical Society: Washington, DC, USA, Vol. 1089, pp. 1–13. [CrossRef]

[6]Barsi, J.A., Lee, K., Kvaran, G., Markham, B.L., Pedelty, J.A., 2014, The spectral response of the Landsat-8 operational land imager, Remote Sens. 6 : 10232–10251, https://doi.org/10.3390/ rs61010232.

[7]Blatchford, M.L., Karimi, P., Bastiaanssen, W.G.M., Nouri, H., 2018, From Global Goals to Local Gains—A Framework for Crop Water Productivity. ISPRSInt. J. Geo.-Inf. 7, 414. [CrossRef]

[8]Change, C., 2016, Agriculture and Food Security. The State of Food and Agriculture; FAO (Ed.) FAO: Rome, Italy. https://eas-et.org/wp-content/uploads/2022/02/Agricalture-and-Food-Security.pdf. Accessed on December. 2, 2023.

[9]El-Bably, A.Z., Abd Allah, A.A., Meleha, M.I., 2007, Influence of field submergence depths on rice productivity in North Delta, Egypt. Alex. J. Agric. Res. 52 (2) 29-35.

[10]FAO., ITPS., 2015, Status of the World's Soil Resources (SWSR) - Main Report. Rome, Italy, Food and Agriculture Organization of the United Nations and Intergovernmental Technical Panel on Soils. http://www.alice.cnptia.embrapa.br/alice/handle/doc/1034770. Accessed on December 2, 2024.

[11]Gómez de Barreda, D., Pardo, G., Osca, J.M., Catala-Forner, M., Consola, S., Garnica, I., López-Martínez, N., Palmerín, J.A., Osuna, M.D., 2021, An Overview of Rice Cultivation in Spain and the Management of Herbicide-Resistant Weeds. Agronomy, 11, 1095. [CrossRef]

[12]González-Betancourt, M., Mayorga-Ruíz, Z.L., 2018, Normalized difference vegetation index for rice management in El Espinal, Colombia. DYNA, 85, 47–56. [CrossRef].

[13]Guan, S., Fukami, K., Matsunaka, H., Okami, M., Tanaka, R., Nakano, H., Sakai, T., Nakano, K., Ohdan, H., Takahashi, K., 2019, Assessing Correlation of High-Resolution NDVI with Fertilizer Application Level and Yield of Rice and Wheat Crops Using Small UAVs. Remote Sens. 11, 112. [CrossRef]

[14]Imran, H.A., Gianelle, D., Rocchini, D., Dalponte, M., Martín, M.P., Sakowska, K., Wohlfahrt, G., Vescovo, L., 2020, VIS-NIR, RedEdge and NIR-Shoulder Based Normalized Vegetation Indices Response to Co-Varying Leaf and Canopy Structural Traits in Heterogeneous Grasslands. Remote Sens. 12, 2254. [CrossRef]

[15]Irmak, S., Odhiambo, L.O., Eisenhauer, D.E., 2013, Irrigation efficiency and uniformity, and crop water use efficiency. Extension Bulletin EC732. University of Nebraska-Lincoln.

[16]Jensen, M.E., 1968, Water consumption by agricultural plants. In: Kozlowski TT (ed) Water deficits and plant growth, vol 2. Academic, New York, pp. 1–45.

[17]Laounia, N., Abderrahmane, H., Abdelkader, K., Zahira, S., Mansour, Z., 2017, Evapotranspiration and Surface Energy Fluxes Estimation Using the Landsat-7 Enhanced Thematic Mapper Plus Image over a Semiarid Agrosystem in the North-West of Algeria. Rev. Bras. Meteorol. 32, 691–702. [CrossRef]

[16]Magliulo, V., d'Andria, R., Rana, G., 2003, Use of the modified atmometer to estimate reference evapotranspiration in Mediterranean environments, Agricultural Water Management, 63: 1-14.

[19]Mirzaee, S., Mirzakhani Nafchi, A., 2023, Monitoring Spatiotemporal Vegetation Response to Drought Using Remote Sensing Data. Sensors 23, 2134. [CrossRef][PubMed]

[20]Odhiambo, L.O., Irmak, S., 2012, Evaluation of the impact of surface residue cover on single and dual crop coefficient for estimating soybean actual evapotranspiration. Agric. Water Manag. 104, 221–234. [CrossRef]

[21]Park, J., Baik, J., Choi, M., 2017, Satellite-based crop coefficient and evapotranspiration using surface soil moisture and vegetation indices in Northeast Asia. CATENA 156, 305–314. [CrossRef]

[22]Pereira, L.S., Allen, R.G., Smith, M., Raes, D., 2015, Crop evapotranspiration estimation with FAO56: Past and future. Agric. Water Manag. 147, 4–20. [CrossRef]

[23]Pokorny, J., 2019, Evapotranspiration. In Encyclopedia of Ecology, 2nd ed.; Elsevier: Amsterdam, The Netherlands, pp. 292–303. [CrossRef]

[24]Pouladi, P., Badiezadeh, S., Pouladi, M., Yousefi, P., Farahmand, H., Kalantari, Z., Yu, D.J., Sivapalan, M., 2021, Interconnected governance and social barriers impeding the restoration process of Lake Urmia. J. Hydrol. 598, 126489. [CrossRef]

[25]Rabatel, G., Gorretta, N., Labbé, S., 2014, Getting simultaneous red and near-infrared band data from a single digital camera for plant monitoring applications: Theoretical and practical study. Biosyst. Eng. 117, 2–14. [CrossRef]

[26]Ringler, C., Zhu, T., 2015, Water Resources and Food Security. Agronomy, 107, 1533–1538. [CrossRef]

[27]Senay, G.B., Friedrichs, M., Singh, R.K., Velpuri, N.M., 2016, Evaluating Landsat 8 evapotranspiration for water use mapping in the Colorado River Basin. Remote Sens. Environ. 185, 171–185. [CrossRef].

[28]Taherparvar, M., Pirmoradian, N., 2018, Estimation of Rice Evapotranspiration Using Reflective Images of Landsat Satellite in Sefidrood Irrigation and Drainage Network. Rice Sci. 25, 111–116. [CrossRef]

[29]Xing, N., Huang, W., Xie, Q., Shi, Y., Ye, H., Dong, Y., Wu, M., Sun, G., Jiao, Q., 2020, A Transformed Triangular Vegetation Index for Estimating Winter Wheat Leaf Area Index. Remote Sens. 12, 16. [CrossRef]

[30]Xue, J., Su, B., 2017, Significant remote sensing vegetation indices: A review of developments and applications. J. Sens. Article ID:1353691. [CrossRef]

[31]Yang, Y., Feng, Z., Huang, H.Q., Lin, Y., 2008, Climate-induced changes in crop water balance during 1960–2001 in Northwest China. Agric. Ecosyst. Environ. 127, 107–118. [CrossRef]

[32]Zampieri, M., Ceglar, A., Manfron, G., Toreti, A., Duveiller, G., Romani, M., Rocca, C., Scoccimarro, E., Podrascanin, Z., Djurdjevic, V., 2019, Adaptation and sustainability of water management for rice agriculture in temperate regions: The Italian case-study. Land Degrad Dev. 30, 2033–2047. [CrossRef]

[33]Zampieri, E., Pesenti, M., Nocito, F.F., Sacchi, G.A., Valè, G., 2023, Rice Responses to Water Limiting Conditions: Improving Stress Management by Exploiting Genetics and Physiological Processes. Agriculture, 13, 464. [CrossRef]

[34]Zheng, H., Cheng, T., Li, D., Zhou, X., Yao, X., Tian, Y., Cao, W., Zhu, Y., 2018, Evaluation of RGB, Color-Infrared and Multispectral Images Acquired from Unmanned Aerial Systems for the Estimation of Nitrogen Accumulation in Rice. Remote Sens. 10, 824. [CrossRef]